Journal of Polymer Research **11:** 9–21, 2004.

Synthesis and Characterization of New Polyimides Based on 3,6-Bis(4-aminophenoxy)benzonorbornane

Sheng-Huei Hsiao* and Tai-Lin Huang
Department of Chemical Engineering, Tatung University, 40 Chungshan North Road, 3rd Section, Taipei, Taiwan, R.O.C.
(Author for correspondence; Tel.: +886-2-25925252 ext. 2977; Fax: +886-2-25861939; E-mail: shhsiao@ttu.edu.tw)*

Received 20 May 2003; accepted in revised form 18 September 2003

Key words: benzonorbornane, dietheramine, high-performance polymer, polyimide, structure-property relations

Abstract

A novel benzonorbornane-based dietheramine monomer, 3,6-bis(4-aminophenoxy)benzonorbornane (BAPBN), was prepared in two steps from aromatic nucleophilic chloro-displacement reaction of *p*-chloronitrobenzene with the potassium phenolate of 3,6-dihydroxybenzonorbornane, followed by hydrazine catalytic reduction of the intermediate dinitro compound. A series of benzonorbornane-based polyimides were prepared from the diamine BAPBN with various aromatic dianhydrides via a conventional two-stage synthesis in which the poly(amic acid)s obtained in the first stage were heated stage-by-stage at 150∼300 °C to give the polyimides. The intermediate poly(amic acid)s had inherent viscosities between 0.58 and 2.03 dL/g. Almost all the solution-cast poly(amic acid) films could be thermally converted into flexible and tough polyimide films with good tensile properties. Some polyimides with more flexible backbones exhibited good solubility in polar organic solvents. Depending on the structures of the dianhydrides, the glass-transition temperatures (T_g) of these polyimides were recorded between 209 and 327 °C by differential scanning calorimetry (DSC) or dynamic mechanical analysis (DMA), and the softening temperatures (T_s) determined by thermomechanical analysis (TMA) stayed in the 197∼320 °C range. Decomposition temperatures for 10% weight loss all occurred above 480 °C in both air and nitrogen atmospheres. The polyimides also showed low dielectric constants (2.62–3.53 at 1 MHz). For the comparative purpose, a series of corresponding polyimides based on l,4-bis(4-aminophenoxy)benzene (BAPB) was also prepared and characterized.

Introduction

Aromatic polyimides are a class of high-performance polymers that have many desirable properties such as high glass transition temperatures (T_g), low dielectric constants, excellent mechanical properties, high chemical resistance, and high thermo-oxidative stability [1, 2]. Some of these materials have been widely used in industry as structural materials and integrated circuit insulators. However, one of the problems with most polyimides is their insolubility in most organic solvents and high melting or softening temperatures. This makes it impossible for most polyimides to be directly processed in their imidized forms, thus may narrow down their applicability. Therefore, various efforts have focused on the synthesis of soluble and/or thermoplastic polyimides without much sacrifice of their excellent properties. Typical approaches were to introduce kinks of flexible linkages, noncoplanar units, or bulky lateral groups along the backbone [3–16].

It has been generally recognized that aryl-ether linkage imparts properties such as better solubility and melt-processing characteristics and improved toughness compared to polyimides without aryl-ether linkage. However, the decrease in mechanical properties on heating is almost always a consequence of the reduced chain stiffness or T_g. On the other hand, the attachment of bulky lateral groups can impart an increase in T_g by restricting the segmental mobility, while providing an enhanced solubility due to decreasing packing and crystallinity. Thus, combining these two structural modifications minimized the trade-off between the processability and the useful/positive properties of aromatic polyimides. Previous studies have shown that incorporating both of the benzonorbornane segment and the ether linkage into the backbones of polyamides and polyimides leads to the reduction in crystallization tendency and an improvement in solubility [17–19]. In a continuation of these studies, the present article reports the synthesis and characterization of a new family of polyimides derived from the benzonorbornane-based dietheramine, i.e. 3,6-bis(4-aminophenoxy)benzonorbornane (BAPBN). The solubility in organic solvents, tensile properties, crystallinity, thermal properties, and dielectric properties of the polyimides were investigated. It was hoped that the incorporation of the hindered ether-linked diamine would decrease polymer inter- and intra-molecular interactions and would generally disrupt the co-planarity of aromatic units to reduce the packing efficiency and the crystallinity. This should promote the solubility while maintaining a moderate to high T_g through controlled segmental mobility. The polyimides were also expected to exhibit low dielectric constants because of the

increased free volume and hydrophobicity caused by the fused norbornane group. In addition, analogous polyimides based on 1,4-bis(4-aminophenoxy)benzene (BAPB) were also examined for comparison.

Experimental

Materials

3,6-Dihydroxybenzonorbornane (Acros), potassium carbonate (K_2CO_3) (Fluka), *p*-chloronitrobenzene (Tokyo Chemical Industry; TCI), 10% palladium on charcoal (Pd/C) (Fluka), and hydrazine monohydrate (Acros) were used as received. *N*,*N*-Dimethylacetamide (DMAc) (Fluka) was purified by distillation under reduced pressure over calcium hydride and stored over 4 Å molecular sieves. One of the diamine monomers, 1,4-bis(4-aminophenoxy)benzene (BAPB) (TCI), was used without further purification. Commercially available aromatic tetracarboxylic dianhydrides such as pyromellitic dianhydride (PMDA) (Aldrich) and 3,3′,4,4′-benzophenonetetracarboxylic dianhydride (BTDA) (Aldrich) were purified by recrystallization from acetic anhydride. 3,3′,4,4′-Diphenylsulfonetetracarboxylic dianhydride (DSDA) (New Japan Chemical Co.), 4,4′-oxydiphthalic dianhydride (ODPA) (Oxychem), 3,3′,4,4′-biphenyltetracarboxylic dianhydride (BPDA) (Oxychem), and 2,2-bis(3,4-dicarboxyphenyl)hexafluoropropane dianhydride (6FDA) (Hoechst Celanese) were purified by heating in vacuo at 250 °C for 3 h prior to use. As described in our previous publications [20–26], the bis(ether anhydride)s that included 1,4-bis(3,4-dicarboxyphenoxy)benzene dianhydride (HQDA; mp = 264–266 °C) [20], 1,4-bis(3,4-dicarboxyphenoxy)-2-*tert*-butylbenzene dianhydride (*t*-BuHQDA; mp = 211–213 °C) [21], 1,2-bis(3,4-dicarboxyphenoxy)benzene dianhydride (CADA; mp = 187–188 °C) [22], 1,5-bis(3,4-dicarboxyphenoxy)naphthalene dianhydride (1,5-NDODA; mp = 252–253 °C) [23], 2,3-bis(3,4-dicarboxyphenoxy)naphthalene dianhydride (2,3-NDODA; mp = 264–265 °C) [22], 2,7-bis(3,4-dicarboxyphenoxy)naphthalene dianhydride (2,7-NDODA; mp = 165–166 °C) [24], 2,2-bis[4-(3,4-dicarboxyphenoxy)phenyl]propane dianhydride (BPADA; mp = 182–184 °C) [25], and 2,2-bis[4-(3,4-dicarboxyphenoxy)phenyl]hexafluoropropane dianhydride (BPAFDA; mp = 226–228 °C) [26], were prepared in three main steps starting from the nucleophilic nitro-displacement reaction of 4-nitrophthalonitrile with the respective aromatic diol precursors followed by alkaline hydrolysis of the intermediate bis(ether dinitrile)s and dehydration of the resultant bis(ether-dicarboxylic acid)s.

Monomer Synthesis

3,6-Bis(4-nitrophenoxy)benzonorbornane (BNPBN)

In a 500-mL round-bottomed flask, 14.7 g (0.084 mol) of 3,6-dihydroxybenzonorbornane and 26.5 g (0.168 mol + 0.1 g) of *p*-chloronitrobenzene were dissolved in 120 mL of dry DMF. Then, 23.1 g (0.168 mol) of potassium carbonate was added, and the suspension solution was refluxed at 140∼150 °C for 6 h. After cooling, the mixture was poured into 800 mL of methanol/water (1 : 1 by volume), and the precipitated light yellow solid was collected by filtration, and washed thoroughly with methanol and water. The yield of the product was 33.0 g (94% yield). The crude product was recrystallized from DMF/methanol to afford 25.6 g (73% yield) of light yellow crystals (mp = 183–185 °C).

IR (KBr): 1513 (N=O asymmetric stretch), 1342 (N=O symmetric stretch), 1226 cm^{-1} (C–O stretch). ^1H NMR (399.65 MHz, DMSO-d_6, δ): 8.26 (d, H_f, 4H), 7.17 (d, H_e, 4H), 7.03 (s, H_a, 2H), 3.29 (s, H_b, 2H), 1.80, 1.12 (d, H_d, 4H), 1.71, 1.47 (d, H_c, 2H). ^{13}C NMR (99 MHz, DMSO-d_6, δ): 164.76 (C^7), 145.69 (C^2), 143.39 (C^{10}), 142.92 (C^3), 127.30 (C^9), 121.52 (C^8), 117.53 (C^1), 48.90 (C^4), 41.03 (C^6), 25.29 (C^5).

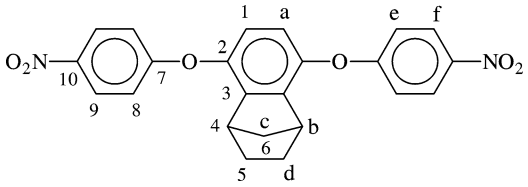

ELEM. ANAL. Calcd. for $C_{23}H_{18}N_2O_6$(418.41): C, 66.03%; H, 4.34%; N, 6.69%. Found: C, 66.20%; H, 4.31%; N, 6.63%.

3,6-Bis(4-aminophenoxy)benzonorbornane (BAPBN)

A mixture of the obtained dinitro compound (25.6 g, 0.061 mol), 10% Pd/C (0.2 g), ethanol (200 mL), and hydrazine monohydrate (20 mL) was heated at reflux temperature for about 10 h. The resultant clear, darkened solution was filtered to remove catalyst. The filtrate was poured into 200 mL of water to give an off-white powder (18 g, 82% yield) that was isolated by filtration and dried in vacuo at 120 °C for 12 h (mp = 175–176 °C).

IR (KBr): 3421, 3343 (N–H stretch), 1224, 1203 cm^{-1} (C–O stretch). ^1H NMR (399.65 MHz, $CDCl_3$, δ): 6.80 (d, H_e, 4H), 6.62 (d, H_f, 4H), 6.55 (s, H_a, 2H), 3.46 (s, H_b + $-NH_2$, 6H), 1.79, 1.18 (d, H_d, 4H), 1.69, 1.40 (d, H_c, 2H). ^{13}C NMR (99 MHz, $CDCl_3$, δ): 152.84 (C^2), 148.25 (C^7), 143.31 (C^{10}), 141.69 (C^3), 120.47 (C^8), 118.83 (C^1), 117.71 (C^9), 49.59 (C^4), 41.03 (C^6), 26.62 (C^5).

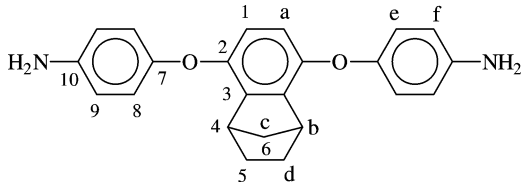

ELEM. ANAL. Calcd. for $C_{23}H_{22}N_2O_2$(358.44): C, 77.07%; H, 6.19%; N, 7.82%. Found: C, 76.90%; H, 6.14%; N, 7.73%.

Polyimide Synthesis

The polyimides were synthesized from various dianhydrides and either the diamine BAPBN or BAPB via a two-step

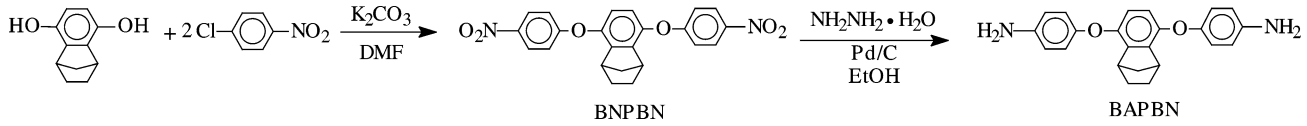

Scheme 1. Preparation of 3,6-bis(4-aminophenoxy)benzonorbornane.

method. The synthesis of polyimide 6FDA/BAPBN is used as an example to illustrate the general synthetic route used to produce the polyimides. To a solution of 0.3632 g (1.013 mmol) of diamine BAPBN in 9.5 mL of CaH_2-dried DMAc in a 50-mL flask, 0.6368 g (1.013 mmol) of dianhydride 6FDA was added in one portion. Thus, the solid content of the solution is approximately 10 wt%. The mixture was stirred at ambient temperature for about 3 h to afford a highly viscous poly(amic acid) solution. The inherent viscosity of the resulting poly(amic acid) was 1.66 dL/g, measured in DMAc at a concentration of 0.5 g/dL. The polymer solution was diluted with 5 mL of DMAc and then poured into a 9-cm glass culture dish, which was placed in a 90 °C oven for removal of the casting solvent. The semi-dried poly(amic acid) film was further dried and converted to the polyimide by sequential heating at 150 °C for 30 min, 200 °C for 30 min, 250 °C for 30 min, and 300 °C for 1 h. The polyimide film was released from the glass substrate upon cooling.

Measurements

Elemental analyses were made on a PerkinElmer 2400 CHN analyzer. IR spectra were recorded on a Horiba FT-720 Fourier transform infrared (FTIR) spectrometer. ^{1}H and ^{13}C NMR spectra were measured on a JEOL EX 400 spectrometer with $CDCl_3$ or DMSO-d_6 as the solvent and tetramethylsilane as the internal reference. The inherent viscosities of the poly(amic acid)s were measured with an Ubbelohde viscometer at 30 °C. An Instron universal tester model 1130 with a load cell of 5 kg was used to study the stress-strain behavior of the polyimide film samples. A gauge length of 2 cm and a crosshead speed of 5 mm/min were used for this study. Measurements were performed at room temperature with film specimens (0.5 cm wide, 6 cm long, and about 70–90 μm thick), and an average of at least five individual determinations was used. Wide-angle X-ray diffraction (WAXD) measurements were performed at room temperature (ca. 25 °C) on a Siemens Kristalloflex D5000 X-ray diffractometer, using nickel-filtered Cu K radiation (= 1.5418 Å, operating at 40 kV and 20 mA). The scanning rate was 3°/min over a range of 2θ = 5–45 °. Thermogravimetric analysis (TGA) was conducted with a TA Instruments TGA 2050. Experiments were carried out on approximately 10 mg of samples in flowing nitrogen (flow rate 100 cm^3/min) at a heating rate of 20 °C/min. Differential scanning calorimetry (DSC) analyses were performed on a PerkinElmer differential scanning calorimeter DSC 7 coupled to a PerkinElmer thermal analysis controller TAG 7/DX at a scan rate of 20 °C/min in flowing nitrogen (20 cm^3/min). Glass transition temperatures (T_g) were read at the middle of the transition in the heat capacity and were taken from the second heating scan after quick cooling from 400 °C at a cooling rate of 200 °C/min. Thermomechanical analysis (TMA) was conducted with a PerkinElmer TMA 7 instrument. The TMA experiments were conducted from 40 °C to 300 °C at a scan rate of 10 °C/min using a penetration probe 1.0 mm in diameter under an applied constant load of 10 mN. Softening temperatures (T_s) were taken as the onset temperature of probe displacement on the TMA traces. DMA experiments were carried out on a TA instruments DMA 2980 dynamic mechanical analyzer. The frequency was set 1 Hz, and the heating rate was 5 °C/min. Relaxation temperatures were determined from corresponding peak top temperatures seen on the damping (tan δ) curves. Dielectric property of the polymer films was tested by the parallel-plate capacitor method using a HP-4194A impedance/gain phase analyzer. Gold electrodes were vacuum deposited on both surfaces of dried films. Experiments were performed at 25 °C in a dry chamber.

Results and Discussion

Monomer Synthesis

The new diamine BAPBN was prepared via a two-step process, as shown in Scheme 1. The first step of this procedure is an aromatic nucleophilic substitution reaction of 3,6-dihydroxybenzonorbornane with *p*-chloronitrobenzene producing the dinitro compound BNPBN, which is subsequently reduced by hydrazine and Pd/C to afford the diamine, BAPBN.

The structures of the dinitro compound BNPBN and the diamine BAPBN were confirmed by elemental analyses as well as FTIR and NMR spectroscopy. Figure 1 shows the FTIR spectra of BNPBN and BAPBN. Absorption bands representative of the nitro functionality were identified by the asymmetrical stretch at 1587 cm^{-1} and the symmetrical stretch at 1342 cm^{-1}. After reduction, the aromatic primary amine absorptions at 3415, 3342, and 3226 cm^{-1} were identified and the bands for the nitro group were absent. The bands around 1240 cm^{-1}, representative of the C–O stretch, were also apparent in both FTIR spectra of BNPBN and BAPBN.

The structures were also confirmed by high-resolution NMR spectra. Figure 2 illustrates the ^{1}H NMR and ^{13}C NMR spectra of diamine BAPBN. Assignments of each carbon and proton also are given in the figures, and these spectra are in good agreement with the proposed molecular structures. In the BNPBN ^{1}H NMR spectrum, the aromatic protons (H_f) at the *ortho* position to the nitro group have the largest chemical shift (8.26 ppm) due to the inductive and anisotropic deshielding effects of the nitro group. There are two chemical shifts in the BAPBN ^{1}H NMR spectrum,

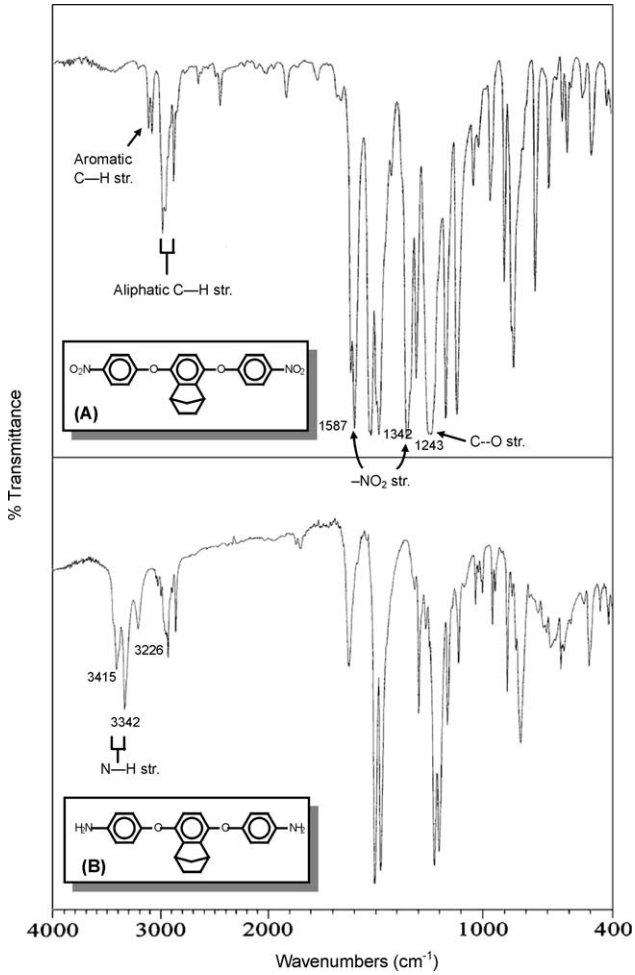

Figure 1. IR spectra of (A) dinitro compound BNPBN and (B) diamine BAPBN.

which assisted in determining the completion of the reduction and the identification of the diamine. The primary aromatic amine protons appear at 3.46 ppm and an AB doublet at 6.62 ppm denotes the aromatic protons *ortho* to the amino group. The chemical shift at 8.26 ppm was absent in the spectrum of BAPBN, indicating that the dinitro compound BNPBN was quantitatively reduced. The aliphatic protons on the benzonorbornane moiety resonate at higher fields. In BAPBN, the two methine protons of H_b resonate as a two-proton singlet at 3.46 ppm. No appreciable coupling between H_b and H_c or H_d indicates that the dihedral angles between them are around 90°. The nonequivalent protons in each methylene group are coupled with each other and show up in the spectrum as an AB system. The doublets (J_{ae} = 8 Hz) of the methylene group *c* are centered at 1.69 and 1.40 ppm; those of methylene *d* are centered at 1.79 and 1.18 ppm, but cannot specifically be assigned to which proton of the methylene group. In the ^{13}C-NMR spectra, upfield shifts of the aromatic carbon resonance, especially for the carbons *para* (C^7) and *ortho* (C^9) to the amino group, were observed for diamine BAPBN because of the resonance effect caused by the electron-donating amino group.

Polymer Synthesis

The polyimides were prepared by the reaction of diamine BAPB or BAPBN with various dianhydrides to form the poly(amic acid)s followed by thermal imidization (Scheme 2). As shown in Table 1, the inherent viscosities of the poly(amic acid) precursors were in the range of 0.58–2.70 dL/g. The resulting thermally imidized polyimide films were transparent and pale yellow in colour. The BTDA/BAPB polyimide yielded a badly cracked film because a high degree of crystallinity developed during thermal imidization, as evidenced by its WAXD pattern. The other BAPB-based polyimides and all the BAPBN-based polyimides afforded tough and flexible films. Even though the BPAFDA-derived polyimides had the lower viscosities (0.58–0.67 dL/g) in the poly(amic acid) stage, they gave quite flexible and strong films.

The conversion of the poly(amic acid) to the fully cyclized polyimide could be monitored by FTIR, ^{1}H NMR, and DSC. Figure 3 shows the IR and ^{1}H NMR spectra of 6FDA/BAPBN polyimide. The complete conversion of *o*-carboxyl amide to the imide ring was evidenced by the disappearance of the amic acid bands at 1650–1700 cm^{-1} and 2500–3500 cm^{-1}, together with the appearance of characteristic imide absorption bands at 1783 (asymmetrical C=O stretch), 1720 (symmetrical C=O stretch), 1380 (C–N stretch), 1100, and 720 cm^{-1} (imide ring deformation). The complete imidization of the poly(amic acid) was also confirmed by the fact that the ^{1}H NMR spectrum showed no residual resonance in the region of 9–11 ppm, indicating the absence of amide NH protons. The multiple sets of resonance peaks between 6.88 and 8.17 ppm are assigned to the aromatic protons. The aliphatic protons appear at 3.36 ppm and in the region of 1.13–1.82 ppm. DSC also was used to investigate cyclization to the imide structure. A strong endotherm corresponding to conversion of the poly(amic acid) to the polyimide started at temperatures around 140 °C and continued for another 100 °C. The complete cyclodehydration occurred before 250 °C during the DSC scan.

Polymer Characterization

Organo-solubility

The solubility behavior of the polyimides was tested qualitatively, and the results are listed in Table 1. As can be seen, except for 6FDA/BAPB, BPAFDA/BAPB (of which the dianhydrides possess the hexafluoroisopropylidene linkage), and 2,3-NDODA/BAPB (of which the dianhydride exhibits *ortho*-linked naphthalene units), the other BAPB-based polyimides are insoluble in all six of the organic solvents tested. However, several of the BAPBN-based polyimides are soluble in aprotic polar solvents at room temperature or upon heating. Some of them are even soluble in less efficient *m*-cresol and THF. This improvement in the organo-solubility of these polyimides can be attributed to the incorporation of pendent fused norbornane structures, which disrupt the close packing of the polymer chains and decrease the interchain interactions. Thus, the introduction of ben-

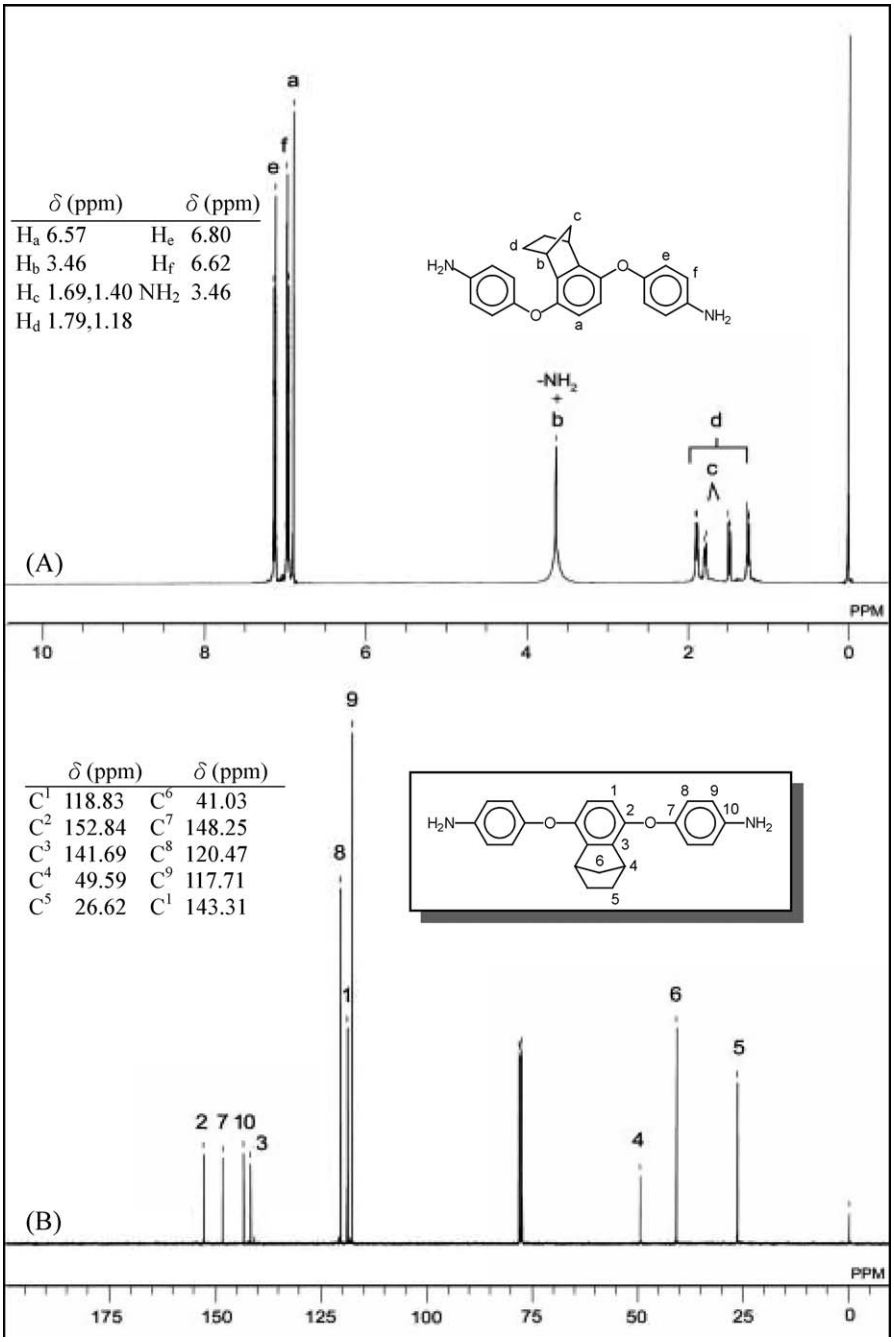

Figure 2. ^{1}H NMR (A) and ^{13}C NMR (B) spectra of diamine BAPBN in $CDCl_3$.

zonorbornane together with flexible ether links is effective in producing organo-soluble polyimides.

Tensile Properties

The tensile properties of the film samples of all polyimides except BTDA/BAPB are also summarized in Table 1. The polymer films had tensile strengths of 84∼123 MPa, elongations to break of 8∼42%, and tensile moduli of 1.7∼2.5 GPa. In most cases, the BAPBN-based polyimides revealed a higher ultimate tensile strength and modulus, but a smaller extension to break than the corresponding BAPB-based polyimides. The stress-strain curves and low elongations to break for the BAPBN-based polyimides are indicative of brittle fracture; the polymer films, however, were creasable without cracking. The relatively lower extensibility may be attributable to the presence of the pendent fused norbornane groups, which may result in a less effective uncoiling the molecular segments in response to an applied force.

X-ray Diffraction Data

All the polyimide films were characterized by wide-angle X-ray diffraction studies. The diffraction patterns of some typical BAPB- and BAPBN-based polyimides are illustrated in Figure 4. The results revealed that the BTDA/BAPB polyimide had a relatively higher degree of crystallinity, and

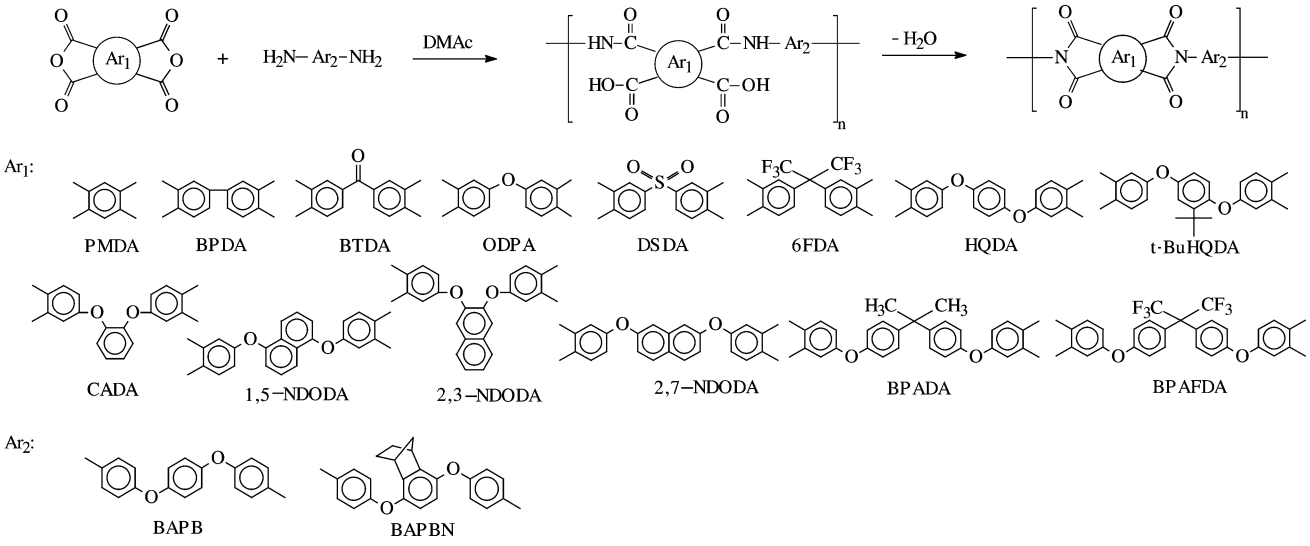

Scheme 2. Preparation of polyimides.

Table 1. Inherent viscosities, solubility behaviors, and tensile properties of polyimides

Sample	η inh[a] (dl/g)	Solubility[b]						Tensile strength (MPa)	Elongation to break (%)	Tensile modulus (GPa)
		NMP	DMAc	DMF	DMSO	*m*-Cresol	THF			
PMDA/BAPB	2.70	−	−	−	−	−	−	104	16	2.2
PMDA/BAPBN	2.03	−	−	−	−	−	−	113	11	2.4
BPDA/BAPB	1.94	−	−	−	−	−	−	119	17	2.5
BPDA/BAPBN	1.91	−	−	−	−	−	−	121	13	2.2
BTDA/BAPB	1.81	−	−	−	−	−	−	−[c]	−	−
BTDA/BAPBN	1.51	δ	−	−	−	−	−	114	9	2.5
ODPA/BAPB	1.03	−	−	−	−	−	−	114	11	2.3
ODPA/BAPBN	1.10	+h	+h	−	δ	+h	−	111	9	2.4
DSDA/BAPB	1.31	−	−	−	−	−	−	111	18	2.2
DSDA/BAPBN	1.27	+	+	+	+h	+h	−	120	10	2.4
6FDA/BAPB	1.27	δ	δ	+	−	+h	+	103	16	2.1
6FDA/BAPBN	1.66	+	+	+	+h	+h	+	123	11	2.3
HQDA/BAPB	0.94	−	−	−	−	−	−	107	9	2.5
HQDA/BAPBN	0.88	δ	−	δ	δ	+	−	92	10	2.0
t-BuHQDA/BAPB	1.32	−	δ	δ	−	+h	δ	105	20	1.9
t-BuHQDA/BAPBN	1.01	+h	δ	+h	−	+h	+	103	8	1.7
CADA/BAPB	1.63	δ	−	δ	−	+h	−	94	32	1.9
CADA/BAPBN	1.50	+	+	δ	−	+	+	113	8	2.4
1,5-NDODA/BAPB	1.14	−	−	−	−	−	−	113	21	2.0
1,5-NDODA/BAPBN	1.27	−	−	−	−	−	−	123	13	2.2
2,3-NDODA/BAPB	1.82	+	+	+h	δ	+	+h	97	42	1.9
2,3-NDODA/BAPBN	1.52	+	+	+h	+h	+	+h	112	11	2.2
2,7-NDODA/BAPB	1.52	−	−	−	−	−	−	95	8	1.8
2,7-NDODA/BAPBN	1.32	+h	δ	−	−	+h	−	91	10	2.1
BPADA/BAPB	0.97	−	−	−	−	+h	−	95	19	1.8
BPADA/BAPBN	0.95	+	+	+	δ	+	+	99	9	2.1
BPAFDA/BAPB	0.67	+h	δ	−	−	−	−	86	11	1.7
BPAFDA/BAPBN	0.58	+	+	+	δ	+	+	84	9	1.8

[a]Inherent viscosity of the poly(amic acid) precursor measured at a concentration of 0.5 g/dl in DMAc at 30 °C.
[b]Qualitative solubility tested with 10 mg of sample in 1 ml of the solvent. +: soluble at room temperature; δ: partially soluble; +h: soluble on heating at 100 °C; −: insoluble even on heating.
[c]Too brittle to be tested.

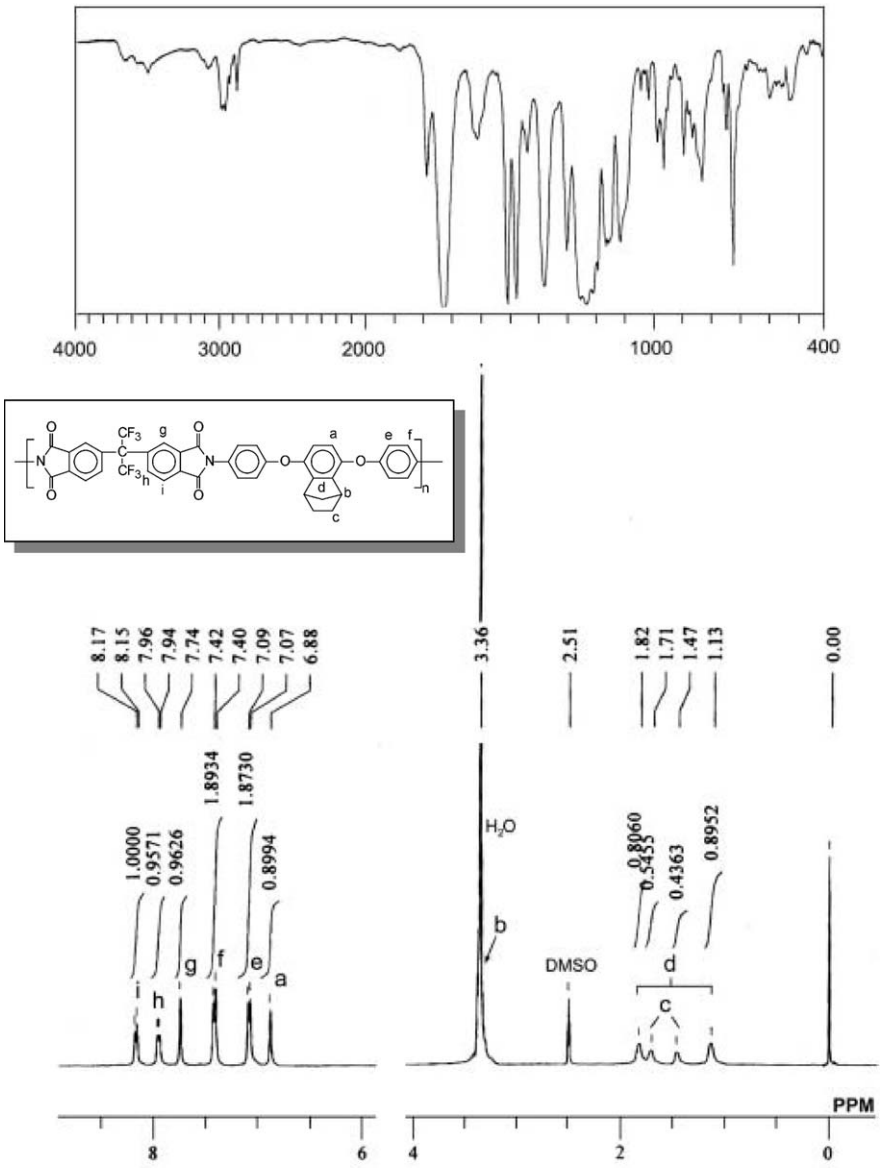

Figure 3. The typical set of IR and ^{1}H NMR (in DMSO-d_6) spectra of 6FDA/BAPBN polyimide.

the PMDA/BAPB and ODPA/BAPB polyimides exhibited a somewhat reduced level of crystallinity as compared to the BTDA-derived polyimide, whereas all of the others showed amorphous patterns. The introduction of bulky pendent norbornane moiety disrupts the backbone symmetry and interferes with the tight packing of the polymer chains; thus, all the BAPBN-based polyimides showed almost completely amorphous diffraction patterns.

Glass Transition and Softening Temperatures

The T_gs of the polyimides were first measured using DSC. The heat capacity jump is generally obvious in DSC heating diagrams. Only four polymers, such as PMDA/BAPB, BPDA/BAPB, BTDA/BAPB, and PMDA/BAPBN, showed no discernible heat capacity jump. The T_g values are listed in Table 2 for these two series of films. Only one BAPB-based polyimide (with HQDA) of all exhibited the melting endotherm in the first DSC heating traces before 400 °C. The HQDA/BAPB polyimides showed a clear melting endothermic peak around 381 °C. Rapid cooling and reheating showed T_g at 218 °C and disappearance of the melting transition. In general, both molecular packing and chain rigidity affect T_g. It is reasonable that the polymers with bis(ether anhydride) CADA have the lowest T_g in both BAPB- and BAPBN-based polyimide series due to the flexible ether linkages and the less linear *ortho*-linked units. In contrast, the polymers derived from dianhydrides without hinge units (such as PMDA and BPDA) or with stiffer (such as 6FDA) or polar hinges (such as DSDA and BTDA) have the higher T_g values. In most cases, especially for those from ether-containing dianhydrides, the introduction of the pendent fused norbornane group resulted in only small changes in the T_g values obtained from DSC analyses. Thus, the increased rotational barrier caused by the voluminous substituents may be overcame by the effect of asymmetry and increased free

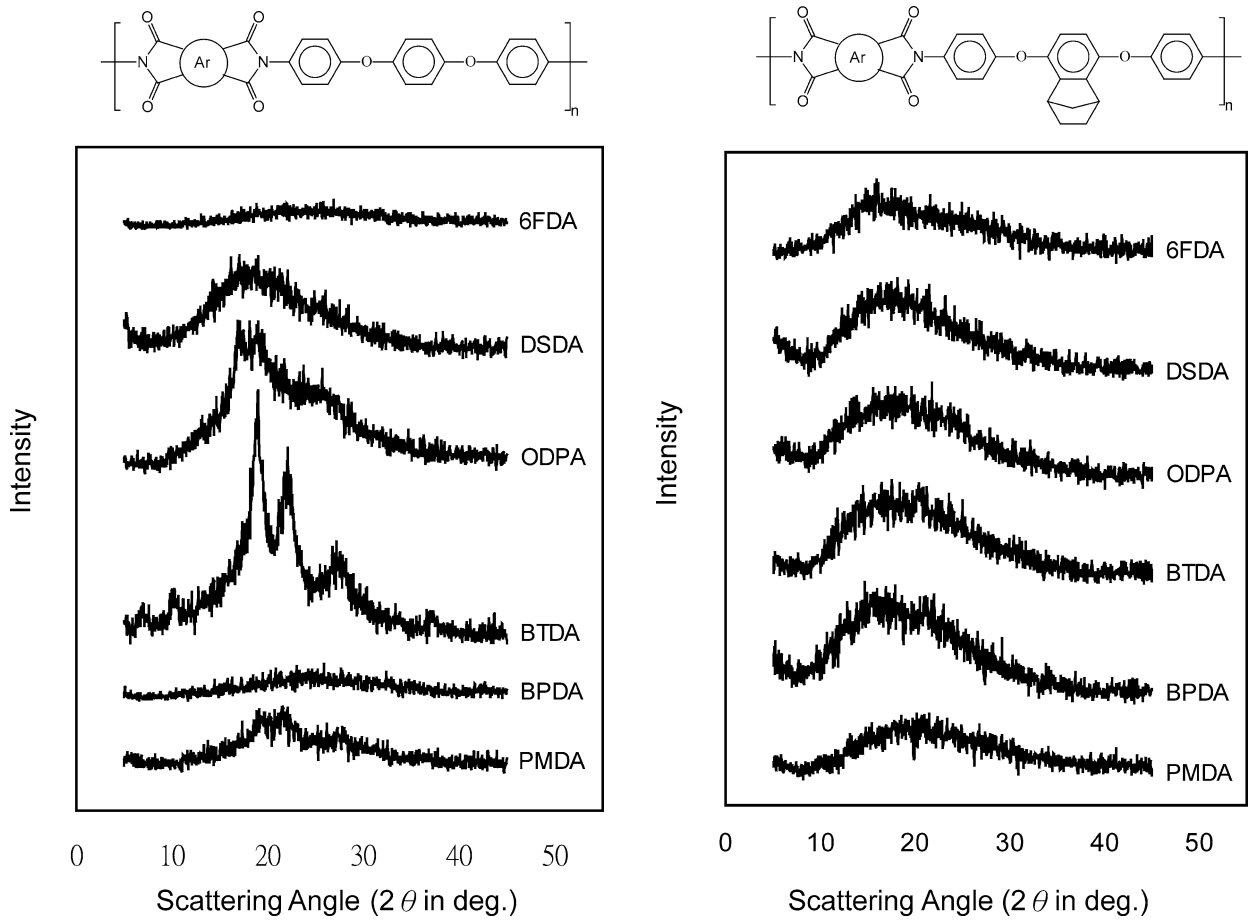

Figure 4. X-ray diffraction patterns of some BAPB and BAPBN polyimides.

volume introduced with the pendent group, which is likely to reduce packing efficiency and interchain interactions and should lessen T_g.

The softening temperatures (T_s) (may be referred as apparent T_g) of the polyimide films were determined by the TMA method using a loaded penetration probe. They were read from the onset temperature of the probe displacement on the TMA trace. As can be seen from Table 2, in most cases the T_s values obtained by TMA are comparable to the T_g values measured by the DSC experiments. The trend of T_s variation with the chain stiffness is similar to that of T_g observed in the DSC measurements. In almost all cases, the BAPBN-based polyimides have similar T_s values to those for the BAPB-based analogues. Exceptions are BTDA/BAPBN and DSDA/BAPBN, where T_s values are lower by 41 and 27 °C than the corresponding BTDA/BAPB and DSDA/BAPB. The relatively lower T_s value for the DSDA/BAPBN polyimide may indicate that it exhibits a higher degree of plasticity near T_g than its analogous DSDA/BAPB polyimide without norbornane groups. An interesting comparison is between the TMA traces of the semicrystalline BTDA/BAPB polyimide and the amorphous BTDA/BAPBN polyimide (Figure 5). The difference in temperature dependence of the probe displacement of these two polymers clearly indicates the difference in their molecular mobility beyond T_g. The probe on the BTDA/BAPBN film showed a faster and deeper penetration starting at about 241 °C attributed to a faster weakening of interchain interactions as the temperature increased.

Viscoelastic Relaxation Behaviors

The polyimides obtained from commercially available dianhydrides, such as PMDA, BPDA, BTDA, ODPA, DSDA, and 6FDA, were subjected to DMA experiments. Two relaxation processes can be observed above room temperature for both the BAPB- and BAPBN-based polyimide films. DMA results of PMDA/BAPBN and BPDA/BAPB are chosen as examples and are shown in Figures 6 and 7, respectively. The β relaxation processes were observed in the range from room temperature to 200 °C, possibly due to the local molecular motions related to the diamine constituent of the polymer chain. The high temperature relaxation is an α-relaxation process. The α relaxation corresponds to the glass transition while the β relaxation is a sub-glass transition process. The glass relaxation temperatures (obtained from tan δ_{max} data) at 1 Hz also are shown in Table 2. These data are generally in good agreement with T_g values obtained from DSC.

Thermal and Thermo-oxidative Stability

Thermal and thermo-oxidative stabilities of these polyimides were evaluated under both nitrogen and air atmospheres us-

Table 2. Thermal properties of polyimides

Polymer code	T_g (°C)[a]		T_s[b] (°C)	T_d[c] (°C)		Char yield[d] (%)
	First run	Second run		N_2	Air	
PMDA/BAPB	[e]	(330)[f]	313	597	589	61
PMDA/BAPBN		(327)	320	514	507	62
BPDA/BAPB		(275)	268	589	579	63
BPDA/BAPBN	253	266 (275)	267	525	525	63
BTDA/BAPB		(315)	302	580	574	60
BTDA/BAPBN	247	257 (255)	241	511	504	63
ODPA/BAPB		248 (250)	235	577	575	56
ODPA/BAPBN	240	244 (248)	235	505	513	57
DSDA/BAPB	282	284 (285)	281	532	560	53
DSDA/BAPBN	264	273 (279)	254	482	484	49
6FDA/BAPB	277	281 (281)	275	570	558	58
6FDA/BAPBN	269	271 (271)	269	524	518	56
HQDA/BAPB	216 (381)[g]	218	215	582	574	53
HQDA/BAPBN	220	224	215	509	523	54
t-BuHQDA/BAPB	234	236	229	539	527	55
t-BuHQDA/BAPBN	233	236	224	492	495	61
CADA/BAPB	203	206	193	561	568	52
CADA/BAPBN	196	206	193	505	513	53
1,5-NDODA/BAPB	234	244	240	573	559	59
1,5-NDODA/BAPBN	235	248	226	518	527	66
2,3-NDODA/BAPB	207	224	225	572	573	60
2,3-NDODA/BAPBN	227	228	222	509	528	60
2,7-NDODA/BAPB	231	233	224	560	570	57
2,7-NDODA/BAPBN	231	235	227	509	528	57
BPADA/BAPB	207	211	205	525	521	52
BPADA/BAPBN	207	209	197	508	521	57
BPAFDA/BAPB	218	220	212	546	522	56
BPAFDA/BAPBN	219	221	215	508	513	57

[a]Midpoint temperature of baseline shift on the DSC heating trace (rate 20 °C/min). Second run: the subsequent run after rapid cooling from 400 °C at −200 °C/min.
[b]Softening temperature measured by TMA (penetration method) with a constant applied load of 10 mN at a heating rate of 10 °C/min.
[c]Decomposition temperature at which a 10% weight loss was recorded by TGA at a heating rate of 20 °C/min.
[d]Residual weight % at 800 °C in nitrogen.
[e]No discernible transitions was observed.
[f]Values in the parentheses are the temperatures at tan δ_{max} on the DMA curves.
[g]A medium-intensity melting endotherm with peak top temperature at 381 °C.

ing a 10 wt% loss values (T_d) for comparison. Typical TGA curves for polyimides PMDA/BAPBN and PMDA/BAPB are reproduced in Figure 8 and Figure 9, respectively. The T_d values for the BAPB-based polyimides ranged from 532 to 597 °C in nitrogen and 521 to 589 °C in air, values compared to those of commercial polyimides. The T_d values for the BAPBN-based polyimides stayed in the range of 482–524 °C in nitrogen and 484–528 °C in air, which are reasonable considering the less stable aliphatic segments. In some cases the T_d values in air were slightly higher than that in nitrogen, possibly because of the oxidative crrosslinking, or an early weight-gained oxidation of the aliphatic groups when thermally degraded in air.

Dielectric Property

The measurements of the dielectric constants were performed between gold layers: the polyimide film was dried carefully, and a thin gold layer was vacuum deposited on both surfaces of the polymer film. This procedure excludes any contact problems. Table 3 gives the results of some polyimides obtained from commercially available dianhydrides. From the data in Table 3 it can be seen that the BAPBN-based polyimides generally exhibit lower dielectric constants compared with the corresponding BAPB-based analogs and standard polyimides such as PMDA/ODA polyimide. The decreased dielectric constants might be attributed to two factors: the bulkiness of the pendent norbornane group, resulting in less packing efficiency and increased free volume, and the aliphatic nature of the norbornane segment, resulting in an increased hydrophobicity and deareased polarity. In addition, the strong electronegativity of fluorine results in very low polarizability of the C–F bonds, thus further decreasing the dielectric constant. Hence, the 6FDA/BAPBN exhibited the lowest dielectric constant (2.62 at 1 MHz).

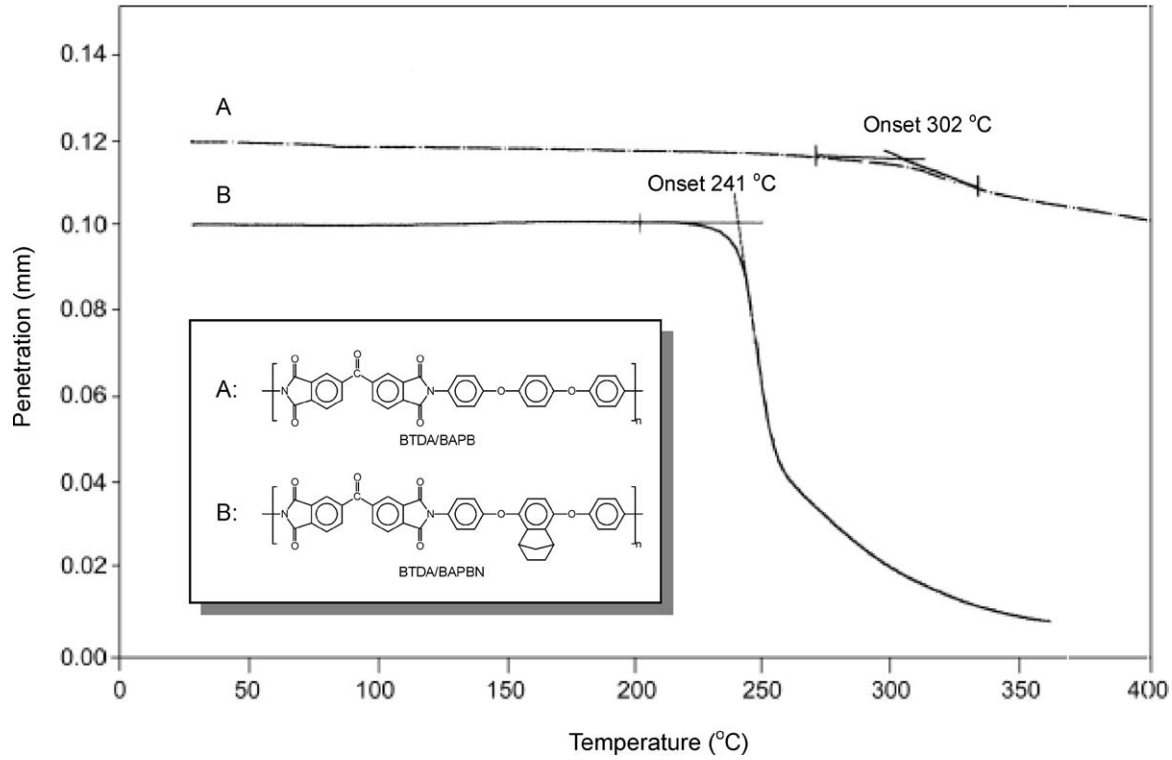

Figure 5. TMA thermograms of polyimides BTDA/BAPB and BTDA/BAPBN. Heating rate = 10 °C/min; DC force = 10 mN.

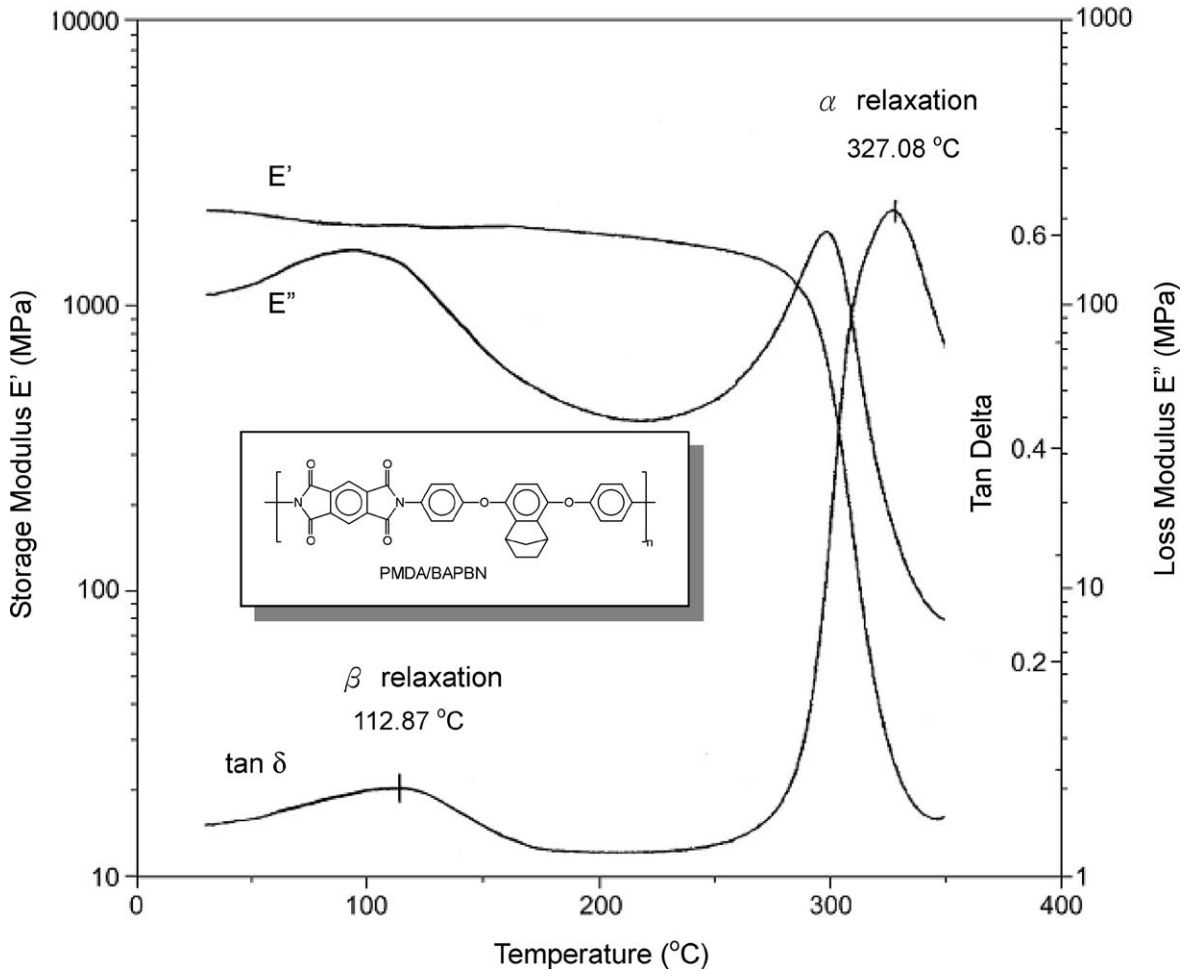

Figure 6. DMA curves of the PMDA/BAPBN polyimide. Sample size = 14 × 5 × 0.08 mm; Amplitude = 30 μm; Autotension = 125%; Frequency = 1 Hz; Scan rate = 5 °C/min.

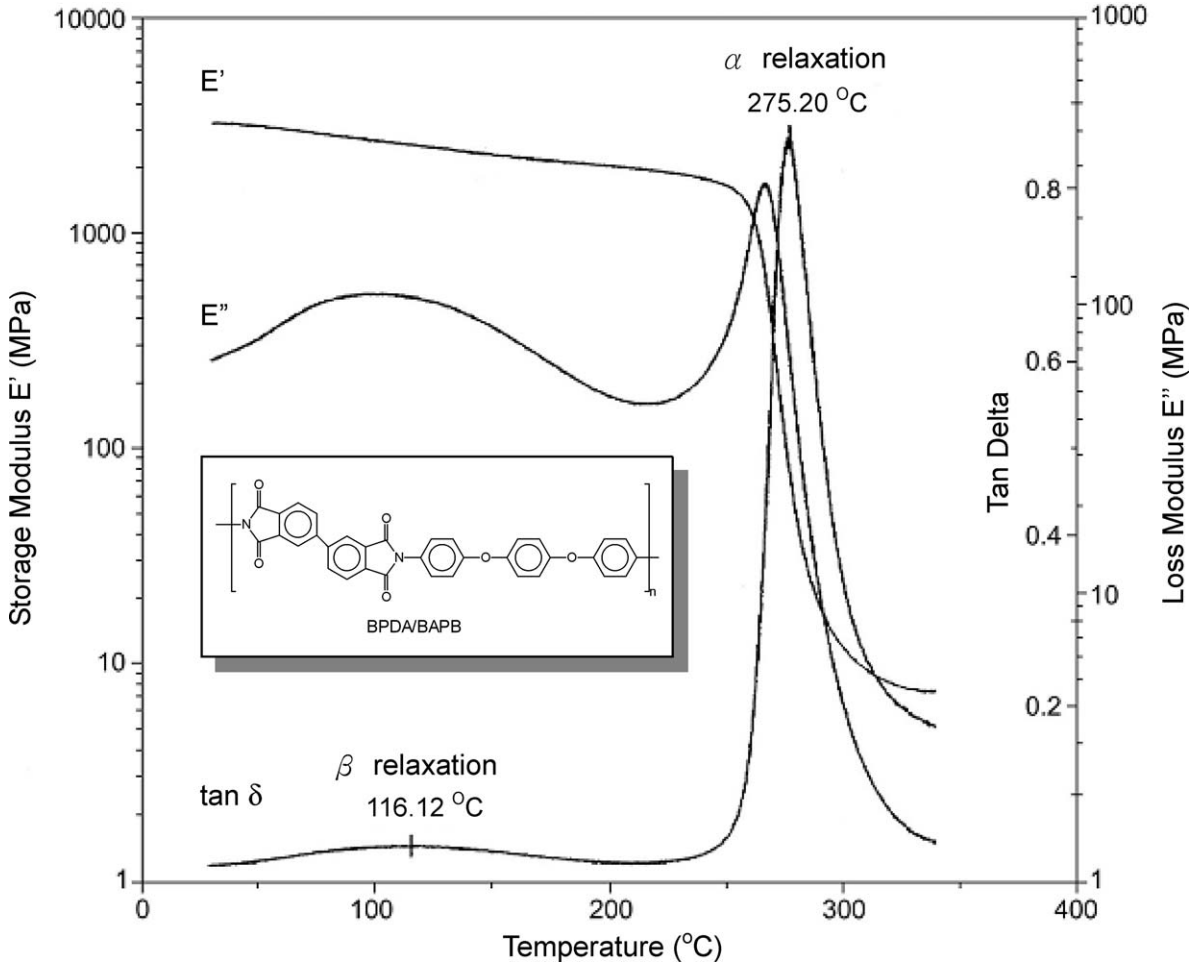

Figure 7. DMA curves of the BPDA/BAPB polyimide. Sample size = 14 × 5 × 0.07 mm; Amplitude = 30 μm; Autotension = 125%; Frequency = 1 Hz; Scan rate = 5 °C/min.

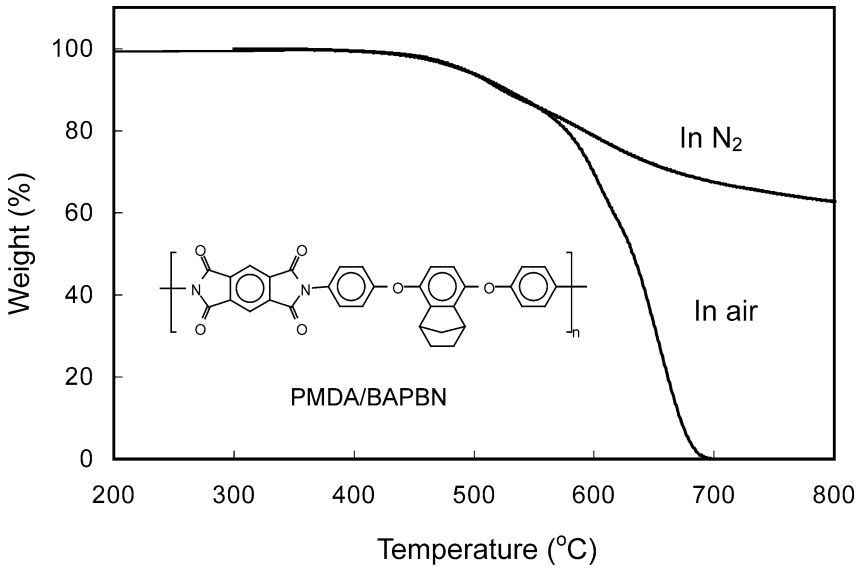

Figure 8. TGA curves of PMDA/BAPBN polyimide (Heating rate = 20 °C/min).

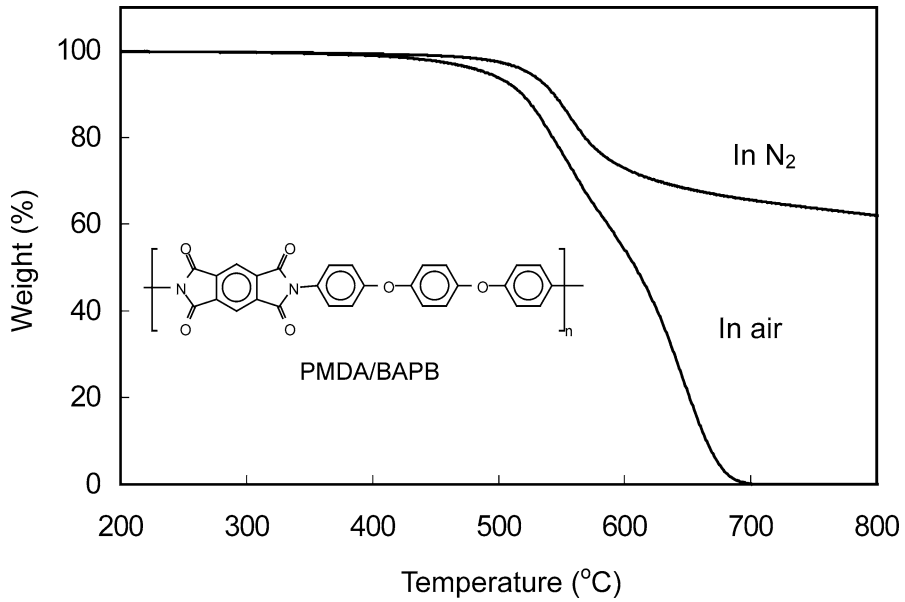

Figure 9. TGA curves of PMDA/BAPB polyimide (Heating rate = 20 °C/min).

Table 3. Dielectric constant of some polyimide films

Polymer	Dielectric constant, dry			
	1 kHz	10 kHz	1 MHz	40 MHz
PMDA/BAPB	3.46	3.46	3.37	3.39
PMDA/BAPBN	3.22	3.22	3.12	3.20
BPDA/BAPB	3.27	3.30	3.24	3.27
BPDA/BAPBA	2.97	2.97	2.91	2.96
BTDA/BAPB	3.36	3.36	3.30	3.36
BTDA/BAPBN	3.30	3.30	3.24	3.28
ODPA/BAPB	3.08	3.10	3.05	3.07
ODPA/BAPBN	2.84	2.85	2.80	2.85
DSDA/BAPB	3.69	3.69	3.62	3.65
DSDA/BAPBN	3.60	3.60	3.53	3.61
6FDA/BAPB	2.85	2.85	2.82	2.84
6FDA/BAPBN	2.68	2.68	2.62	2.64
PMDA/ODA[a]	3.62	3.66	3.54	3.54

[a]A reference polyimide prepared from PMDA and 4,4′-oxydianiline (ODA) (η_{inh} of the poly(amic acid) precursor = 2.50 dl/g).

Conclusions

3,6-Bis(4-aminophenoxy)benzonorbornane has been prepared in high purity and high yield from an aromatic nucleophilic displacement reaction of 3,6-dihydroxybenzonorbornane and *p*-chloronitrobenzene followed by hydrazine Pd/C-catalyzed reduction. A series of new polyimides have been synthesized from this diamine and various aromatic dianhydrides and bis(ether anhydride)s. These polyimides were essentially amorphous and showed good mechanical properties and thermal stability. The introduction of pendent fused norbornane groups onto the polyimide backbones generally led to an enhanced organo-solubility and lowered dielectric constants without an unacceptable detriment to their thermal properties.

Acknowledgements

The authors are grateful to the National Science Council of the Republic of China for its financial support.

References

1. D. Wilson, H. D. Stenzenberger and P. M. Hergenrother, Eds., *Polyimides*, Blackie, Glasgow and London, 1990.
2. M. K. Ghosh and K. L. Mittal, Eds., *Polyimides: Fundamentals and Applications*, Marcel Dekker, New York, 1996.
3. T. Takekoshi, J. E. Kochanowski, J. S. Manello and M. J. Webber, *J. Polym. Sci., Polym. Symp.*, **74**, 93 (1986).
4. G. C. Eastmond and J. Paprotny, *React. Funct. Polym.*, **30**, 27 (1996).
5. G. C. Eastmond and J. Paprotny, *J. Mater. Chem.*, **7**, 589 (1997).
6. G. C. Eastmond, M. Gibas and J. Paprotny, *Eur. Polym. J.*, **35**, 2097 (1999).
7. S. Tamai, A. Yamaguchi and M. Ohta, *Polymer*, **37**, 3683 (1996).
8. Y.-T. Chern and H.-C. Shiue, *Macromolecules*, **30**, 4646 (1997).
9. F. Li, S. Fang, J. J. Ge, P. S. Honigfort, J.-C. Chen, F. W. Harris and S. Z. D. Cheng, *Polymer*, **40**, 4571 (1999).
10. F. Li, J. J. Ge, P. S. Honigfort, S. Fang, J.-C. Chen, F. W. Harris and S. Z. D. Cheng, *Polymer*, **40**, 4987 (1999).
11. S.-H. Hsiao and C.-T. Li, *Macromolecules*, **31**, 7213 (1998).
12. G.-S. Liou, *J. Polym. Sci., Part A: Polym. Chem.*, **36**, 1937 (1998).
13. G.-S. Liou, M. Maruyama, M. Kakimoto and Y. Imai, *J. Polym. Sci., Part A: Polym. Chem.*, **36**, 2021 (1998).
14. D.-J. Liaw, B.-Y. Liaw and C.-M. Yang, *Acta Polym.*, **50**, 332 (1999).
15. D. Ayala, A. E. Lozdno, J. de Abajo and J. G. de la Campa, *J. Polym. Sci., Part A: Polym. Chem.*, **37**, 804 (1999).
16. D. S. Reddy, C.-F. Shu and F.-I. Wu, *J. Polym. Sci., Part A: Polym. Chem.*, **40**, 262 (2002).
17. S.-H. Hsiao and T.-L. Huang, *Polym. J.*, **34**, 225 (2002).
18. S.-H. Hsiao and T.-L. Huang, *J. Polym. Sci., Part A: Polym. Chem.*, **40**, 947 (2002).
19. S.-H. Hsiao and T.-L. Huang, *J. Polym. Sci., Part A: Polym. Chem.*, **40**, 1712 (2002).
20. S.-H. Hsiao and L.-R. Dai, *J. Polym. Sci., Part A: Polym. Chem.*, **37**, 665 (1999).
21. C.-P. Yang, S.-H. Hsiao and H.-W. Yang, *Macromol. Chem. Phys.*, **201**, 409 (2000).
22. S.-H. Hsiao, C.-P. Yang and K.-Y. Chu, *Macromolecules*, **30**, 165 (1997).

23. S.-H. Hsiao, C.-P. Yang and K.-Y. Chu, *Macromol. Chem. Phys.*, **198**, 2153 (1997).
24. S.-H. Hsiao, C.-P. Yang and K.-Y. Chu, *J. Polym. Sci., Part A: Polym. Chem.*, **35**, 2281 (1997).
25. S.-H. Hsiao and P.-C. Huang, *J. Polym. Res.*, **4**, 183 (1997).
26. S.-H. Hsiao and C.-H. Yu, *Polym. J.*, **29**, 944 (1997).